

# Contacts Dynamics across Jamming in a granular glass experiment

C. Coulais,<sup>1</sup> R. P. Behringer,<sup>2</sup> and O. Dauchot<sup>3</sup>

<sup>1</sup>*SPHYNX/SPEC, CEA-Saclay, URA 2464 CNRS, 91 191 Gif-sur-Yvette, France*

<sup>2</sup>*Department of Physics and Center for Nonlinear and Complex Systems,  
Duke University, Durham, North Carolina 27708-0305, USA*

<sup>3</sup>*EC2M, ESPCI-ParisTech, UMR Gulliver 7083 CNRS, 75005 Paris, France*

We study experimentally the vicinity of the Jamming transition by investigating the statics and the dynamics of the contact network of an horizontally shaken bi-disperse packing of photo-elastic discs. Compressing the packing very slowly, while maintaining a mechanical excitation, we produce a granular glass, namely a frozen structure of vibrating grains. Nevertheless, we observe in this glass phase a remarkable dynamics of the *contact network*, which exhibits strong dynamical heterogeneities. Such heterogeneities are maximum at a packing fraction  $\phi^*$ , *distinct* and smaller than the jamming packing fraction  $\phi_J$ , which is indicated by the abrupt variation of the average number of contact per particle. We further demonstrate that the "dynamical transition" taking place at  $\phi^*$  originates in the spatial correlation of the coordination number. Our findings are discussed in the light of recent numerical and theoretical studies of thermal soft spheres.

PACS numbers: 45.70.-n 83.80.Fg

At large packing fraction, disordered packings of particles with repulsive contact interactions jam into a rigid state. For frictionless and athermal particles the jamming transition coincides with the onset of isostaticity and a number of geometrical and mechanical quantities exhibit clear scaling laws with the distance to jamming [1]. One prominent signature of jamming is the singular behavior of the average number of contacts per particle  $z - z_J \propto (\phi - \phi_J)^{0.5}$ , where  $z_J = 2d$ ,  $d$  being the space dimension [2, 3]. The distribution of the gaps between particles displays a delta function at zero and a square root decay for increasing gaps, which is key to the singular behavior of the average contact number [4–7].

Although the average coordination number singularity is the hallmark of jamming at zero temperature, its behavior is less clear at finite temperature. Both experimentally [8] and numerically, [6, 8–11] it was observed that the first peak of the partial pair correlation functions has a finite maximum at a packing fraction  $\phi_J(T) > \phi_J(0)$ . This maximum has been interpreted as a vestige of the divergence seen in the pair correlation function at point J, the  $T = 0$  jamming transition. The vicinity of point J has been explored in a mean-field-like replica description of thermal soft and hard spheres [12]. This description recovers all the observed scalings in temperature and packing fraction *but* the square root singularity of the pair correlation function when  $T = 0^+$  and  $\phi = \phi_J^+$ . This discrepancy, together with the onset of a diverging length in the vibrational properties of the jammed state, [13] suggest that larger scale correlations must be taken into account, and calls for a better characterization of the vicinity of point J.

In the present letter, we focus on the *dynamics* of the contact network, a natural quantity of interest as soon as  $T > 0$ , which to our knowledge has not been considered so far. To this aim, we experimentally investigate

a vibrated two-dimensional bi-disperse packing of grains close to its jamming transition. We verify that the structure, in terms of particle neighborhoods, is completely frozen on the experimental time scales, hence justifying the appellation of a granular glass, and we demonstrate the emergence of heterogeneities in the dynamics of the contact network. These heterogeneities are maximum at a packing fraction  $\phi^*$  smaller than the jamming packing fraction  $\phi_J$ , which is signaled by an abrupt variation of the average number of contacts per particle. We further demonstrate that the "dynamical transition" taking place at  $\phi^*$  originates in the spatial correlation of the coordination number.

Our experimental set up (Fig. 1 top) is adapted from [14, 15], and allows us to shake photoelastic discs between two cross-polarizers, thereby accessing the contact and force network [3, 16]. A bi-disperse mixture of 4964 and 3216 polyurethane (PSM-4) discs, of respectively 4mm and 5mm diameter, lies on a flat transparent surface, which oscillates with an amplitude of 1 cm at a frequency of 10 Hz. The grains are confined in a static rectangular cell, for which the position of one horizontal boundary is tuned using a micro-metric piston attached to a force sensor. An LED back-light and a circular polarizing sheet are inserted in the vibrating surface, so that the grains are lighted by transmission. A monochromatic high resolution CCD camera takes two types of images in phase with the vibration. Every odd period, a circular analyzer is inserted by a rotating wheel in the camera field to visualize the photoelastic pattern. From the direct-light images acquired every even period, we obtain the grain positions with a resolution of 0.5% of the mean grain diameter. Standard tracking and tessellation techniques are then used to obtain the dynamics and the structure of the packings. From the cross-polarized images, we estimate the normal force between two neighbors

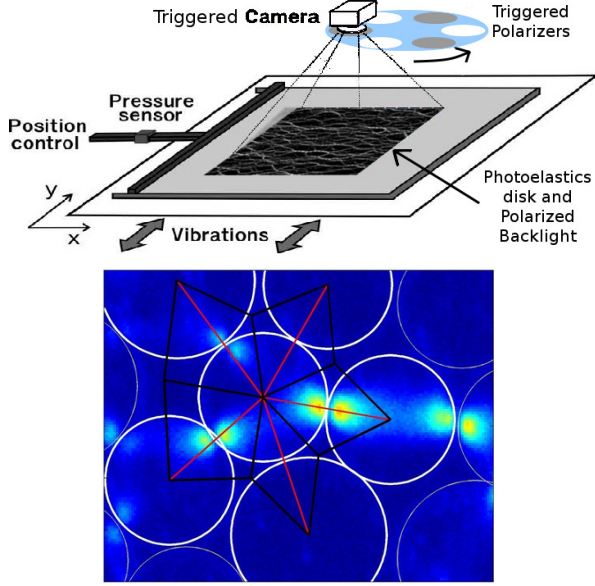


FIG. 1: **Experimental setup.** (color online) **Top:** The vibrating cell. **Bottom:** The photo-elastic pattern at contact. White circles are the grains, red lines the link between neighbors, and dark lines the Delaunay triangulation.

by integrating the square spatial gradient of the light intensity over the area defined by the two Delaunay triangles sharing a common edge (see Fig. 1 bottom). Henceforth, all lengths are expressed in units of the small grains diameter, and time is expressed in units of vibration cycles. Note that as compared to the brass discs, used in [14, 15], the photo elastic discs are much softer (Young modulus of 0.5GPa, as compared to 100GPa).

In order to ensure the highest and most reproducible jammed packings, the packing fraction, which we control within a relative resolution of  $5 \cdot 10^{-6}$  is increased by steps of  $\delta\phi = 3 \cdot 10^{-4}$ , using exponentially increasing time steps (Fig. 2 (top left)). All images are then acquired during stepwise decompression; following a decompression, we fix the packing fraction, and then carefully check that both the pressure – defined as the force measured at the wall normalized by the weight of the grains – and the dynamics are stationary. Fig. 2 (top right) displays the pressure with respect to the packing fraction.  $P_{TOT}$  (respectively  $P_{STAT}$ ) is the pressure measured when the vibration is switched on (respectively off).  $P_{STAT}$  is thus the static pressure sustained by the packing in the absence of vibration, whereas  $P_{DYN} = P_{TOT} - P_{STAT}$  can be interpreted as the additional dynamic pressure, induced by the vibration. At high packing fraction, the pressure is dominated by its static part, whereas at low packing fraction, it is mostly dynamic. A crossover occurs at some intermediate packing fraction, which in [14] was shown to coincide with a maximum in the heterogeneity of the dynamics, as probed at scales of the order of  $10^{-2}$  grain diameters. As compared to the pre-

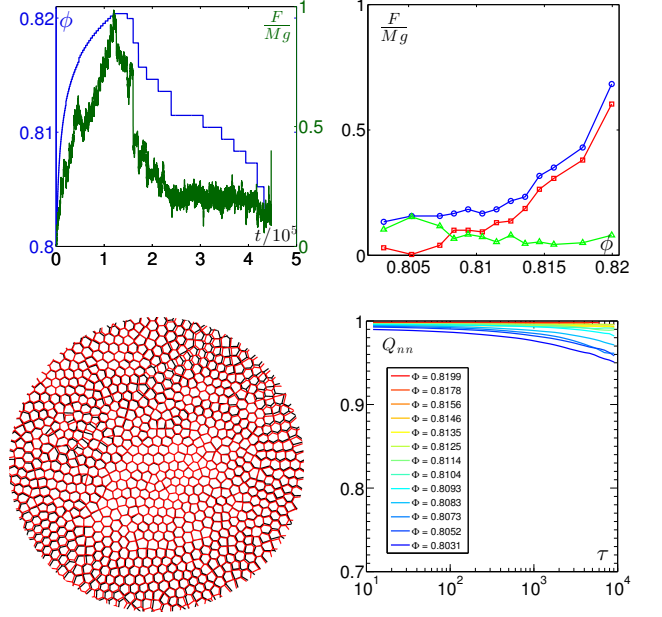


FIG. 2: **Obtaining a granular glass** (color online) **Top Left :** Logarithmic increase followed by a stepwise decrease of the packing fraction, and pressure measured at the wall. **Top Right :** Average pressure vs packing fraction: ( $\circ$ ) :  $P_{TOT}$ , ( $\square$ ):  $P_{STAT}$ , ( $\triangle$ ):  $P_{DYN}$  as defined in the text. **Left:** Superposition of the Laguerre cells computed at times  $t = 1$  and  $t = 5000$  for the loosest packing ( $\phi = 0.8031$ ). **Right:** Average fraction of neighbors  $Q_{nn}(\tau)$  which have not changed between two images separated by a time interval  $\tau$ , for different packing fractions, as indicated in the legend.

vious experiments performed with brass discs, we note two significant differences. First, the transition is shifted to lower values of the packing fraction, a fact which we attribute to the higher interparticle friction of the photo-elastic discs. Second the range of packing fraction on which the pressure varies from say 0.1 to 1 is much larger, ( $[0.800 - 0.820]$ ) as compared to  $[0.840 - 0.845]$ ), a direct evidence of the discs softness.

Altogether, the above compression protocol produces a structure in terms of nearest neighbor relationships, which is completely frozen on experimental timescales. The Laguerre tessellation of two different packings separated by a time lag 5000 can be superimposed almost perfectly, even at the loosest packing fraction (fig. 2 bottom-left). This is further quantified by  $Q_{nn}(\tau)$ , the average fraction of *neighbor* relationships surviving in a time interval  $\tau$ .  $Q_{nn}$  remains larger than 95% even for the loosest packing fraction and barely departs from 1 for the denser ones (fig. 2 bottom-right).

We now turn to the description of the contact network, as provided by the analysis of the photoelastic pictures. A threshold is applied to both the gap between neighboring particles and the contact force, to decide what particles are in contact (Fig. 3 (left) ). There is always

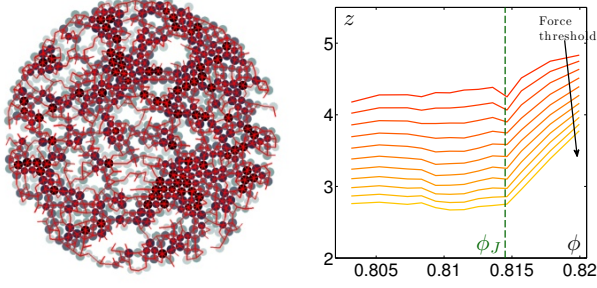


FIG. 3: **Contacts** (color online) **Left:** Map of the coordination number for  $\phi = 0.8125$ , (grayscale level from black – high coordination number – to white – low coordination number. Contacts are indicated in red. **Right:** Average coordination number  $z$  vs. packing fraction  $\phi$ , determined according to various force thresholds

some arbitrariness in the choice of such thresholds and one should keep in mind that the resulting "contact network" is actually the union of the real contacts and very small gaps. Fig. 3 (right) displays the average number of contacts,  $z$ , as a function of the packing fraction for different thresholds. While the absolute value of  $z$  depends on the threshold, the dependance on  $\phi$  is very robust:  $z$  is constant at low packing fractions, displays a kink at some intermediate packing fraction, and thereafter, it increases. The kink occurs at a packing fraction which is independent of the threshold. We interpret this packing fraction as the signature of the crossover to jamming in the presence of vibration and find  $\phi_J = 0.8143 \pm 0.0005$ . Above  $\phi_J$ , the system is jammed and,  $z \sim a(\phi - \phi_J)^\beta + z_c$ , where  $\beta \in [0.4 - 1]$  and  $z_c \in [2.7 - 4.3]$  depend on the threshold. Since counting arguments for frictional packings [1] constrain  $z_c$  between 3 and 4 for two-dimensional systems, it is fair to say that the transition indicated by the kink is robust to the thresholding procedure.

The natural quantity of to characterize the dynamics of contacts is the contact overlap between  $t$  and  $t + \tau$ :

$$Q^z(t, \tau) = \frac{1}{N} \sum_i Q_i^z(t, \tau), \quad (1)$$

where  $Q_i^z(t, \tau) = \Theta(2 - |\delta z_i(t, \tau)|)$ , with  $\Theta(\cdot)$ , the Heavy-side function and  $\delta z_i(t, \tau)$ , the change in number of contact of grain  $i$ , between  $t$  and  $t + \tau$ . Fig. 4 (top left) displays  $Q_z(\tau) = \langle Q^z(t, \tau) \rangle_t$  for the various packing fractions, where  $\langle \cdot \rangle_t$  denotes the time average. The black curve corresponds to the packing fraction of the jamming crossover  $\phi_J$ . For  $\phi > \phi_J$ ,  $Q^z(\tau)$  remains constant at values ranging between 0.7 and 0.9, indicating that there is no long time decorrelation of the contact network. The sole decorrelation observed above  $\phi_J$  occurs at short time. This decorrelation is more significant when  $\phi$  approaches  $\phi_J$  and is presumably related to the density of rattlers, which also increases. More remarkable is the fact that, for  $\phi < \phi_J$ , this short times relaxation saturates, while a long time relaxation clearly sets in. In

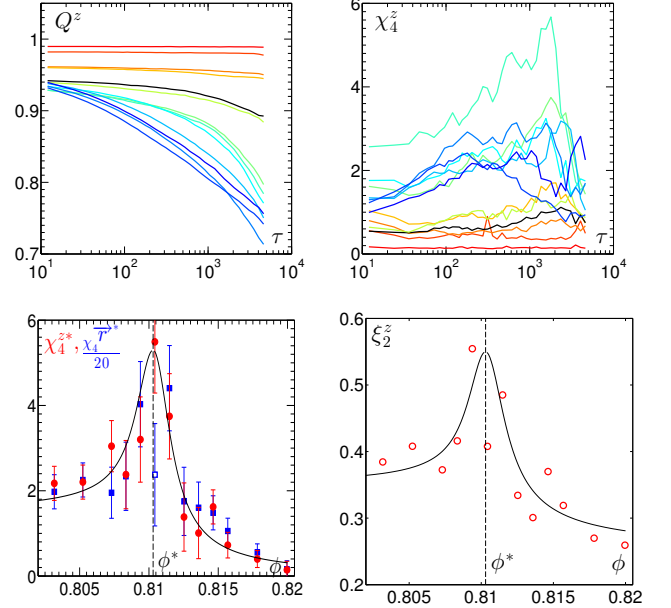


FIG. 4: **Contact Dynamics** (color online). **Top Left:** Average contact overlap  $Q_z(\tau)$  for different packing fractions (same color code as in fig. 2 bottom right with the curve corresponding to  $\phi_J$  plotted in black). **Top Right:** Contact overlap dynamical susceptibility  $\chi_4^z(\tau)$  (same color code). **Bottom Left:** Maximal contact overlap dynamical susceptibility  $\chi_4^{z*}$  (●) versus  $\phi$  and maximal dynamical susceptibility  $\chi_4^{z*}$  (■) versus  $\phi$ , computed from the grain displacements. Note the □ data point, which has an anomalously low value: we interpret it as the signature of a lack of statistics close to the transition, where the timescales of the heterogeneities become extremely large. **Bottom right:** Spatial correlation length  $\xi_2^z$  of the coordination number versus  $\phi$ .

some sense the jamming crossover, signals a transition between a frozen and an evolving contact network, the phenomenology of which is reminiscent of the glass transition scenario [17], except that it concerns the contact network instead of the density profile.

To further characterize this long term dynamics, we compute the dynamical susceptibility (see [18] for an introduction to dynamical heterogeneities):

$$\chi_4^z(\tau) = N \frac{\text{Var}(Q^z(t, \tau))}{\langle \text{Var}(Q_i^z(t, \tau)) \rangle_i}, \quad (2)$$

where the variances are sampled over time and  $\langle \cdot \rangle_i$  denotes the average over the grains. This dynamic susceptibility measures the spatial correlation in the dynamics of the contact network. One sees in Fig. 4 (top right) that  $\chi_4^z(\tau)$  becomes significant for  $\phi < \phi_J$  and then exhibits a maximum  $\chi_4^{z*}$ , which in turn displays a clear maximum at a packing fraction  $\phi^* = 0.810 \pm 0.001$  (Fig. 4 bottom left) : the reorganization of the contacts is maximally collective, indicating a dynamical crossover *below*  $\phi_J$ . When performing the same experiments with brass discs [14, 15], the authors reported a maximum of the

correlations of the dynamics, associated with the particle displacements. More precisely, they computed  $\chi_4^{\vec{r}}(\tau)$  using formula (2), with  $Q_i^z(t, \tau)$  replaced by  $Q_i^{\vec{r}}(t, \tau) = \exp(-\|\vec{r}_i(t + \tau) - \vec{r}_i(t)\|^2 / \sigma^2(\tau))$ . Here,  $\vec{r}_i(t)$  is the position of grain  $i$  at time  $t$ , and  $\sigma(\tau)$  the root mean square displacement of the grains. In the present case (Fig. 4 bottom left),  $\chi_4^{\vec{r}}*$  correlates strongly with  $\chi_4^{z*}$  and in particular also has a maximum at  $\phi^*$ . Quite remarkably  $\chi_4^{\vec{r}}*$  is 20 times larger than  $\chi_4^{z*}$ . This suggests that the correlation is not trivially a one to one correspondence, and calls for further investigations. Furthermore, these dynamical heterogeneities find their root in the static heterogeneity of the contact network. Indeed, computing the spatial correlator of the coordination number (not shown here) we extract a correlation length  $\xi_z$ , which shares the same non-monotonic dependence on  $\phi$ , with a maximum at  $\phi^*$  (Fig. 4 (bottom right)).

Let us now summarize and discuss our observations. Having prepared a granular glass, the neighborhood structure of which is frozen, we have observed two salient features of the contact network: (i) the evolution of the averaged number of contacts with packing fraction,  $z(\phi)$ , points to a first transitional packing fraction  $\phi_J$ ; (ii) the dynamics of the contact network, together with the fluctuation of the coordination number are maximally heterogeneous at a packing fraction  $\phi^* < \phi_J$ . These results clarify those previously obtained in the same setup with brass discs [14]. These authors observed a maximum in the heterogeneities of the dynamics for the packing fraction, where  $P_{DYN}(\phi)$  and  $P_{STAT}(\phi)$  intersects. They were able to attribute their observations to jamming, but they could not precisely identify the underlying mechanism responsible for these heterogeneities. Here, we show that they are associated with the dynamics of the contact network, which in turn is governed by its heterogeneous structure. Note that contacts include both positive overlaps and small gaps between particles.

The existence of a maximal correlation length suggests that the experiment is probing both sides of the jamming transition. In the case of the brass discs, this was a puzzling conclusion, given the very large stiffness of the discs. Our results resolve this apparent paradox by demonstrating that there are several signatures of point J at finite vibration, and that the one associated with the dynamical heterogeneities occurs at a lower packing fraction than the one for which the average number of contact increases. In fact, in the present study,  $P_{DYN} \simeq P_{STAT}$  at  $\phi^*$ .  $\phi_J$  in the case of the brass discs presumably coincides with the very sharp increase of pressure observed in [14] at the largest packing fractions.

Several signatures of point J have also been reported recently in simulations of thermal frictionless soft spheres [6, 9, 11]. Motivated by the observation that the first peak of the partial pair correlation functions exhibits a finite maximum at a packing fraction  $\phi_J(T)$  [8], the authors of [9] showed that at any finite  $T$   $\phi_J(T) < \phi_i(T)$ ,

the isostatic packing fraction where  $z = 2d$ . Recent discussions [19] confirm that, depending on the observable, there are numerous crossover lines meeting at point J at  $T = 0$ . This phenomenology is reminiscent of the so-called Widom lines observed in the supercritical region close to a critical point [20, 21]. Our observations may find an explanation in this kind of scenario. Alternatively, one cannot rule out the possible effect of static friction, which, by adding an extensive number of degrees of freedom to the packing, allows for hyper-static packings at jamming, and can significantly alter the above picture. Future plans are to investigate the role of the vibration magnitude to further elucidate this matter.

We acknowledge L. Berthier and F. Zamponi for illuminating discussions and are grateful to Cécile Wiertel-Gasquet and Vincent Padilla for their skillful technical assistance.

- 
- [1] M. van Hecke, Journal of Physics: Condensed Matter **22**, 033101 (2010).
  - [2] C. S. O'Hern, S. A. Langer, A. J. Liu, and S. R. Nagel, Phys. Rev. Lett. **88**, 075507 (2002).
  - [3] T. S. Majmudar, M. Sperr, S. Luding, and R. P. Behringer, Phys. Rev. Lett. **98**, 058001 (2007).
  - [4] L. E. Silbert, D. Ertas, G. S. Grest, T. C. Halsey, and D. Levine, Phys. Rev. E **65**, 031304 (2002).
  - [5] G. Parisi and F. Zamponi, Rev. Mod. Phys. **82**, 789 (2010).
  - [6] H. Jacquin, L. Berthier, and F. Zamponi, Phys. Rev. Lett. **106**, 135702 (2011).
  - [7] A. Donev, S. Torquato, and F. H. Stillinger, Phys. Rev. E **71**, 011105 (2005).
  - [8] Z. Zhang, N. Xu, D. T. N. Chen, P. Yunker, A. M. Alsayed, K. B. Aptowicz, P. Habdas, A. J. Liu, S. R. Nagel, and A. G. Yodh, Nature **459**, 230 (2009).
  - [9] L. Wang and N. Xu, ArXiv e-prints (2011), 1112.2429.
  - [10] X. Cheng, Phys. Rev. E **81**, 031301 (2010).
  - [11] M. Otsuki and H. Hayakawa, arxiv **1111.1313** (2011).
  - [12] L. Berthier, H. Jacquin, and F. Zamponi, Phys. Rev. E **84**, 051103 (2011).
  - [13] M. Wyart, S. R. Nagel, and T. A. Witten, EPL (Europhysics Letters) **72**, 486 (2005).
  - [14] F. Lechenault, O. Dauchot, G. Biroli, and J. P. Bouchaud, EPL (Europhysics Letters) **83**, 46003 (2008).
  - [15] F. Lechenault, O. Dauchot, G. Biroli, and J. P. Bouchaud, EPL (Europhysics Letters) **83**, 46002 (2008).
  - [16] T. S. Majmudar and R. P. Behringer, Nature **435**, 1079 (2005).
  - [17] P. G. Debenedetti and F. H. Stillinger, Nature **410**, 8 (2001).
  - [18] L. Berthier, G. Biroli, J.-P. Bouchaud, L. Cipelletti, and W. V. Sarloos, eds., *Dynamical Heterogeneities in Glasses, Colloids, and Granular Media* (Oxford University Press, 2011).
  - [19] L. Berthier and F. Zamponi, private communication.
  - [20] H. E. Stanley, *Introduction to Phase Transitions and Critical Phenomena*. (Oxford University Press, 1971).
  - [21] V. V. Brazhkin, Y. D. Fomin, A. G. Lyapin, V. N. Ryzhov, and E. N. Tsiok, J. Phys. Chem. B **115**, 1411214115 (2011).